Evaluation of cerebral microstructural changes in adult patients with obstructive sleep apnea by MR diffusion kurtosis imaging using a whole-brain atlas

Sameer Vyas, Paramjeet Singh, Niranjan Khandelwal, Varan Govind[1], Ashutosh Nath Aggarwal[2], Manju Mohanty[3]

Departments of Radiodiagnosis and Imaging, [2]Pulmonary Medicine and [3]Neurosurgery, Postgraduate Institute of Medical Education and Research, Chandigarh, India, [1]Department of Radiology, University of Miami, Miami, Florida, USA

Correspondence: Dr. Sameer Vyas, Department of Radiodiagnosis and Imaging, Postgraduate Institute of Medical Education and Research, Chandigarh, India. E-mail: sameer574@yahoo.co.in

Abstract

Purpose: The association between obstructive sleep apnea (OSA) and cognitive impairment is well-recognized, but little is known about neural derangements that underlie this phenomenon. The purpose of this study was to evaluate the utility of diffusion kurtosis imaging (DKI) using a whole-brain atlas to comprehensively assess microstructural tissue changes in the brain of patients with OSA. **Methods:** This prospective study was conducted in 20 patients with moderate-to-severe OSA and 20 age- and gender-matched controls. MRI data acquisition was performed with 3 Tesla and data was analyzed using a whole-brain atlas. DKI data were processed and transformed into a brain template space to obtain various kurtosis parameters including axial kurtosis (AK), radial kurtosis (RK), mean kurtosis (MK), and kurtosis fractional anisotropy (KFA) using a 189-region brain atlas in the same template space. These kurtosis measurements were further analyzed using a student *t*-test in order to determine kurtosis measurements that present significant differences between the OSA patient set and the control set. **Results:** Significant differences ($P < 0.05$) were found in AK (54 regions), RK (10 regions), MK (6 regions) and KFA (41 regions) values in patients with OSA as compared to controls. DKI indices, using an atlas-based whole-brain analysis approach used in our study, showed widespread involvement of the anatomical regions in patients with OSA. **Conclusion:** The kurtosis parameters are more sensitive in demonstrating abnormalities in brain tissue structural organization at the microstructural level before any detectable changes appear in conventional MRI or other imaging modalities.

Key words: Kurtosis imaging; MRI; obstructive sleep apnea

Introduction

Obstructive sleep apnea (OSA) is a common yet under-diagnosed sleep-related breathing disorder. OSA

Access this article online	
Quick Response Code:	Website: www.ijri.org
	DOI: 10.4103/ijri.IJRI_326_19

Cite this article as: Vyas S, Singh P, Khandelwal N, Govind V, Aggarwal AN, Mohanty M. Evaluation of cerebral microstructural changes in adult patients with obstructive sleep apnea by MR diffusion kurtosis imaging using a whole-brain atlas. Indian J Radiol Imaging 2019;29:356-63.

Received: 07-Aug-2019 **Revision:** 26-Sep-2019
Accepted: 23-Oct-2019 **Published:** 31-Dec-2019

is clinically characterized by chronically fragmented sleep as well as intermittent hypoxemia. Well-recognized clinical manifestations or associations of OSA include cardiovascular disease, neurocognitive impairment, and impaired metabolic functions.[1,2] Despite substantial evidence of an association between OSA and cognitive impairment, little is known about the tissue structural alterations in brain anatomical regions underlying the impairment.[3-5] Functional MRI studies in OSA patients have shown changes in neural activation that are related to cognitive impairment and autonomic dysfunction; it is likely that these functional changes are due to deficits in tissue structural deficits.[1-3] Neuroimaging studies have given insight into the brain anatomical structures and functions affected in individuals with OSA.[4,5] The neuroimaging methods used in these studies complement more traditional sleep-assessment techniques such as polysomnography or neuropsychological tests. Patients with OSA show brain abnormalities in white matter (WM) and gray matter (GM) using advanced MR imaging techniques such as diffusion tensor imaging (DTI), functional MRI, and magnetic resonance (MR) spectroscopy.[6-8] Diffusion kurtosis imaging (DKI) is an extension of the DTI technique, which allows estimation of the more commonly used diffusion tensor metrics as well as diffusion kurtosis metrics.[9,10]

It is established that water molecular diffusion displacement behavior in a tissue of human organ deviates from a strict Gaussian model that is assumed in DTI, due to the presence of cellular structural barriers and intracellular organelles that hinder free diffusion. In contrast, DKI uses a non-Gaussian model for characterizing water diffusion, thereby providing a more accurate representation of restricted diffusion, which may give additional biomarkers in disease conditions. In contrast to DTI, DKI uses higher b-values and provides additional metrics that are complementary to DTI metrics.[9-10] Few studies have assessed the brain tissue microstructural changes using DTI[11-16] or DKI[17,18] in the patients of OSA. These studies had shown that there are significant microstructural changes in patients of OSA as compared to controls. Previous studies of OSA patients by DKI had been done by using region of interest (ROI)-based analysis with Matlab; however in our study, we used whole-brain atlas analysis with four commonly used DKI parameters (axial kurtosis [AK], radial kurtosis [RK], mean kurtosis [MK], and kurtosis fractional anisotropy [KFA]) in 189 brain ROIs. There is no definitive and clinically useful neuropathologic correlates available for cerebral changes in patients with OSA using conventional brain imaging modalities. Therefore, we evaluated tissue microstructural changes within the brain of patients with OSA using DKI.

Materials and Methods

This was a prospective case-control study, conducted from July 2015 to November 2016, after approval from the institutional ethical committee. Inclusion criteria for the patients included in the study were: recently diagnosed OSA patient via polysomnography, apnea-hypopnea index (AHI) ≥15, treatment native, and without any medications, such as β-blockers, α-agonists. Exclusion criteria included the history of stroke or heart failure, uncooperative patients and those having contraindications to MR examination such as metallic implants. The inclusion criteria for the controls included in the study were: no history of stroke or heart failure and no focal structural lesions on routine MRI. Twenty newly diagnosed patients (age range 22–60 years, 17 males) with moderate to severe OSA and 20 age- and gender-matched healthy controls were included in the study. All participants or their relatives provided informed and written consent before participation.

All subjects were scanned using a 3 Tesla MRI scanner (*Verio*; Siemens Healthcare, Erlangen, Germany), equipped with a 12-channel head coil. A 35-minute protocol included conventional MRI sequences, 3D-T1, and DKI acquisitions. The MRI sequences include fluid-attenuated inversion recovery (FLAIR, TE/TR: 94/9000 ms, 25 slices, 4-mm slice thickness), T2 (spin-echo; TE/TR: 96/6000 ms, 25 slices, 4-mm slice thickness) and T1 (MPRAGE; TE/TR: 3.77/1800 ms, 1 mm^3 isotropic). DKI data were obtained using a single-shot twice-refocused 2D spin-echo echo-planar imaging sequence with TE/TR: 98/8600, contiguous slices with 3 mm thickness, 3 mm isotropic resolution, one signal average, 30 noncollinear diffusion-weighted gradient directions, 3 diffusion weightings (b = 0, 1000, 2000 s/mm^2), generalized autocalibrating partially parallel acquisition (GRAPPA) acceleration factor of 2.0, and an acquisition time of ~9.1 minutes. Both diffusion-weighted (b = 1000, 2000 s/mm^2) and non-diffusion-weighted (b = 0 s/mm^2) data were processed using *diffusion kurtosis estimator* (DKE)[19] and DiffeoMap[20] and analyzed using *ROIEditor*[21] [Figure 1]. Briefly, first, after processing with DKE, we obtained four DKI-based metrics, that is, AK, RK, MK, and KFA. Second, the subject-space FA and b0 images of each subject were registered to a single-subject FA and b0 images (i.e., *Eve* template in Montreal Neurological Institute, i.e., MNI space) using *DiffeoMap*. Third, we transformed the 189-region brain atlas in MNI space to an individual subject space using *DiffeoMap*. Fourth, we used the atlas in each subject's space in *ROIEditor* to obtain data for statistical analyses from 189 ROIs for the four DKI matrices (AK, KFA, RK, and MK).

Statistical analysis

Comparisons of DKI metrics and demographic data between the control group and OSA patients groups were performed using the student's *t*-test. All statistical tests were two-sided and a $P < 0.05$ was considered for significance. The statistical analysis was carried out using SPSS (SPSS Inc., Chicago, IL, version 21.0 for Windows).

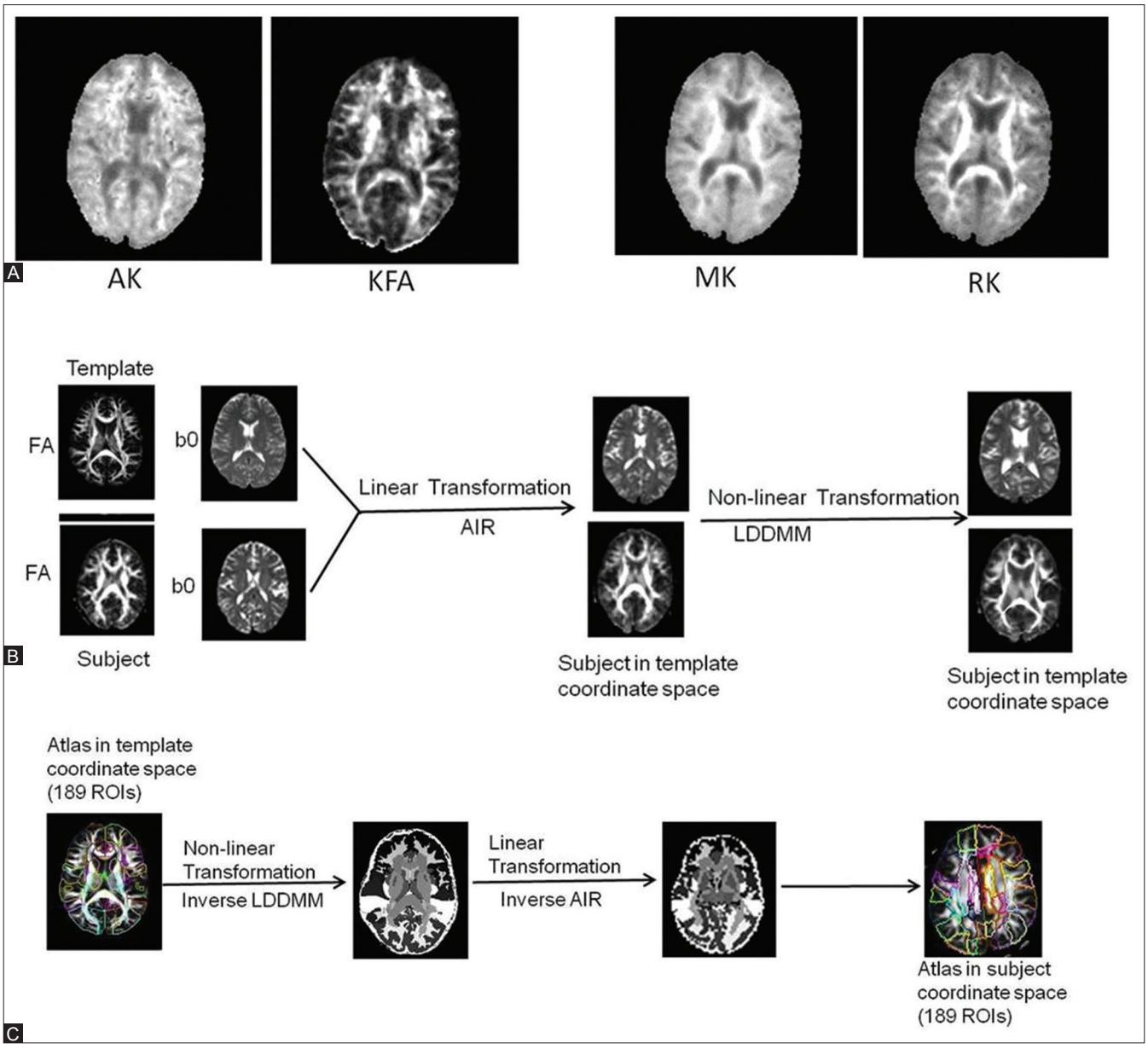

Figure 1 (A-C): Axial kurtosis (AK), kurtosis fractional anisotropy (KFA), mean kurtosis (MK), and radial kurtosis (RK) maps (A) derived from diffusion kurtosis imaging (DKI) at the level of basal ganglia from the subject (from the axial slice 19). Registration of individual subject images to template images (B) in standard coordinate space (i.e., Montreal Neurological Institute space). AIR = automatic image registration used for linear spatial transformation, LDDMM = large deformation diffeomorphic metric mapping used for nonlinear spatial transformation. Transformation of an atlas (*Eve* atlas) in template space (i.e., Montreal Neurological Institute space) to a subject coordinate space (C)

Results

The mean age of the patients and controls was 47.3 years and 44.9 years, respectively. Five patients had moderate sleep apnea (15≤ AHI <30) and 15 patients had severe sleep apnea (AHI ≥30). The majority of the patients showed unremarkable findings on conventional MRI. Multifocal nonspecific periventricular T2 and FLAIR hyperintensities were seen in three patients. One patient showed mild diffuse cerebral cortical atrophy.

AK, RK, KFA, and MK mean values were calculated in 189 brain ROIs in both patients and the control group. Significant differences ($P < 0.05$) in the patient group were found and these include: AK in 54 ROIs [Table 1], KFA in 41 ROIs [Table 2], MK in 6 ROIs [Table 3], and RK in 10 ROIs [Table 4]. Bar diagram of areas from the Eve template in Montreal Neurological Institute (MNI) space showing significant difference between patient and control groups in AK [Figure 2], KFA[Figure 3], MK [Figures 4 and 5].

Table 1: Showing AK values which showed a significant difference between patients and control

Area	Patients		Control		*P*
	Mean	Std. deviation	Mean	Std. deviation	
SFG_PFC_L	0.746	0.057	0.678	0.031	0.000
SFG_PFC_R	0.753	0.110	0.675	0.041	0.005
SFG_pole_L	0.688	0.101	0.563	0.070	0.000
SFG_pole_R	0.758	0.143	0.617	0.049	0.000
MFG_DPFC_L	0.744	0.084	0.646	0.036	0.000
MFG_DPFC_R	0.781	0.134	0.667	0.033	0.001
IFG_orbitalis_L	0.770	0.063	0.717	0.037	0.002
IFG_orbitalis_R	0.822	0.141	0.737	0.030	0.012
IFG_triangularis_L	0.791	0.054	0.748	0.043	0.008
LFOG_L	0.823	0.084	0.753	0.046	0.002
LFOG_R	0.868	0.134	0.755	0.054	0.001
MFOG_L	0.938	0.092	0.820	0.084	0.000
MFOG_R	1.037	0.213	0.821	0.107	0.000
RG_L	0.857	0.081	0.779	0.072	0.002
RG_R	0.847	0.098	0.750	0.071	0.001
PoCG_R	0.668	0.041	0.696	0.039	0.030
MTG_L_pole	0.787	0.064	0.737	0.046	0.007
ITG_L	0.839	0.072	0.797	0.040	0.029
rostral_ACC_L	0.742	0.037	0.702	0.031	0.001
rostral_ACC_R	0.727	0.040	0.699	0.040	0.029
Amyg_L	0.733	0.041	0.705	0.048	0.047
Amyg_R	0.747	0.043	0.718	0.043	0.040
Caud_R	0.676	0.045	0.646	0.041	0.035
Put_L	0.844	0.060	0.777	0.069	0.002
GP_L	0.945	0.075	0.887	0.079	0.021
GP_R	0.980	0.055	0.917	0.088	0.010
Mynert_L	0.864	0.063	0.783	0.078	0.001
Mynert_R	0.829	0.081	0.768	0.075	0.018
NucAccumbens_L	0.834	0.055	0.771	0.071	0.003
NucAccumbens_R	0.783	0.057	0.735	0.079	0.036
Snigra_L	1.015	0.066	0.934	0.069	0.001
Snigra_R	0.968	0.089	0.900	0.111	0.041
CP_L	0.734	0.032	0.700	0.034	0.002
Midbrain_R	0.779	0.057	0.747	0.036	0.038
SCP_L	0.759	0.051	0.726	0.049	0.045
MCP_L	0.911	0.057	0.880	0.036	0.040
ICP_L	0.924	0.083	0.875	0.057	0.036
ICP_R	0.903	0.091	0.850	0.060	0.036
Pons_R	0.912	0.094	0.857	0.052	0.028
Medulla_L	0.853	0.198	0.735	0.094	0.021
ACR_L	0.889	0.045	0.823	0.057	0.000
ACR_R	0.901	0.109	0.826	0.044	0.007
GCC_L	0.703	0.049	0.645	0.046	0.000
GCC_R	0.730	0.057	0.674	0.055	0.003
ALIC_L	0.858	0.040	0.814	0.050	0.004
ALIC_R	0.844	0.042	0.804	0.042	0.005
PLIC_L	0.819	0.036	0.771	0.039	0.000
PLIC_R	0.796	0.038	0.772	0.026	0.024
RLIC_L	0.796	0.054	0.765	0.038	0.040
CGC_L	0.881	0.035	0.853	0.032	0.013
IFO_L	0.787	0.062	0.726	0.053	0.002
AnsaLenticularis_R	0.804	0.059	0.747	0.064	0.005
AnteriorCom_R	0.685	0.072	0.728	0.058	0.046
LenticularFasc_R	0.828	0.059	0.775	0.074	0.016

Contd...

Table 1: Contd...

R=Right; L=Left; SFG=Superior frontal gyrus (posterior segment); PFC=Prefrontal cortex; MFG=Middle frontal gyrus (posterior segment); DPFC=Dorsal prefrontal cortex; IFG=Inferior frontal gyrus; LFOG=Lateral fronto-orbital gyrus; MFOG=Middle fronto-orbital gyrus; RG=Gyrus rectus; PoCG=Postcentral gyrus; MTG=Middle temporal gyrus; ITG=Inferior temporal gyrus; ACC=Anterior cingulate gyrus; Amyg=Amygdala; Caud=Caudate nucleus; Put=Putamen; GP=Globus pallidus; Mynert=Nucleus innominata of Mynert; NucAccumbens=Nucleus accumbens; Snigra=Substancia nigra; CP=Cerebral peduncle; SCP=Superior cerebellar peduncle; MCP=Middle cerebellar peduncle; ICP=Inferior cerebellar peduncle; ACR=Anterior corona radiate; GCC=Genu of corpus callosum; ALIC=Anterior limb of internal capsule; PLIC=Posterior limb of internal capsule; RLIC=Retrolenticular part of internal capsule; CGC=Cingulum (cingulate gyrus); IFO=Inferior fronto-occipital fasciculus; AnsaLenticularis=Ansa lenticularis; AnteriorCom=Anterior commissure; LenticularFasc=Lenticular fasciclus; ENT=Entorhinal area; Ins=Insular; Hippo=Hippocampus; EC=External capsule; CGH=Cingulum (hippocampus); Fx/ST=Fornix (cres)/stria terminalis; SS=Sagittal stratum; LV=Lateral ventricle

Discussion

This prospective study showed that there were significant alterations in many brain anatomical regions for four DKI metrics (i.e., AK, RK, MK, and KFA) in OSA patients. This study was done by using whole-brain atlas analysis template in Montreal Neurological Institute (i.e., MNI space) using DiffeoMap to have more objectivity and uniformity rather than ROI-based analysis done in the previous studies. These findings indicate that microstructural changes occur in specific cerebral regions in the patient group. The observed associations between the regional changes observed by brain imaging metrics and neurocognitive outcomes indicate the anatomical regions with significant structural alterations. Changes in brain morphology of OSA patients have been described in literature.[1-3] However; there is no specific correlation of these nonspecific cerebral changes with OSA, though the complex disease process in OSA may accentuate these cerebral changes. Though conventional MRI may show apparent cerebrovascular changes and cerebral atrophy, it cannot detect subtle vascular and microstructural damages.

We found altered AK values in 54 brain ROIs in the patient group that includes the insula, internal capsule, cingulum, hippocampus, amygdala, dorsolateral pons, and cerebellar peduncles. Our results in the above mentioned anatomical regions agree with the findings of Tummala *et al*. in a group of OSA patients.[17] Moreover, our study found increased AK values in additional anatomical regions in the patient group. We speculate that the higher number of regions with significant AK values in the patient group may be due to either the severity of the patient group enrolled in our study or the data analysis method we used or both. Though most of the areas are bilaterally involved, unilateral involvement is also seen in some of the WM tracts and brainstem. AK values are indicative of the microstructural

Table 2: KFA values which showed a significant difference between patients and control

Area	Patients		Control		*P*
	Mean	Std. deviation	Mean	Std. deviation	
SFG_PFC_L	0.325	0.046	0.282	0.045	0.004
SFG_PFC_R	0.336	0.059	0.291	0.051	0.013
SFG_pole_R	0.309	0.076	0.247	0.057	0.006
MFG_DPFC_L	0.310	0.056	0.252	0.048	0.001
MFG_DPFC_R	0.333	0.070	0.263	0.044	0.001
IFG_orbitalis_R	0.334	0.059	0.283	0.050	0.006
IFG_triangularis_L	0.313	0.047	0.283	0.045	0.048
IFG_triangularis_R	0.297	0.045	0.262	0.046	0.020
RG_L	0.317	0.043	0.286	0.045	0.031
rostral_ACC_L	0.286	0.054	0.249	0.057	0.043
rostral_ACC_R	0.274	0.056	0.236	0.050	0.031
Ins_R	0.221	0.027	0.182	0.040	0.001
Hippo_R	0.262	0.036	0.234	0.039	0.028
Put_L	0.451	0.044	0.381	0.051	0.000
Put_R	0.429	0.060	0.363	0.065	0.002
GP_L	0.423	0.062	0.360	0.058	0.002
GP_R	0.420	0.069	0.364	0.064	0.011
Mynert_L	0.432	0.050	0.385	0.044	0.003
Mynert_R	0.419	0.064	0.369	0.044	0.007
NucAccumbens_L	0.400	0.068	0.357	0.058	0.038
Snigra_L	0.413	0.063	0.357	0.059	0.007
Snigra_R	0.408	0.067	0.361	0.063	0.030
Midbrain_L	0.282	0.035	0.252	0.032	0.006
Midbrain_R	0.272	0.043	0.243	0.035	0.024
MCP_L	0.380	0.050	0.344	0.031	0.009
MCP_R	0.358	0.044	0.324	0.029	0.007
ICP_L	0.358	0.067	0.306	0.042	0.006
ICP_R	0.328	0.056	0.290	0.043	0.021
Medulla_L	0.295	0.059	0.259	0.048	0.041
Medulla_R	0.348	0.054	0.303	0.056	0.013
ACR_R	0.477	0.050	0.439	0.046	0.016
EC_L	0.443	0.053	0.393	0.052	0.005
EC_R	0.420	0.059	0.378	0.067	0.046
CGH_L	0.377	0.049	0.334	0.049	0.008
Fx/ST_L	0.316	0.045	0.276	0.046	0.010
IFO_L	0.457	0.041	0.419	0.049	0.011
SS_L	0.384	0.046	0.355	0.035	0.035
Mammillary_L	0.071	0.020	0.088	0.025	0.020
Mammillary_R	0.064	0.019	0.082	0.019	0.006
LV_frontal_L	0.118	0.024	0.150	0.038	0.003
LV_frontal_R	0.124	0.022	0.149	0.043	0.029

organization of the WM (axons) bundles in the brain. Its direction of change (i.e., increased or decreased compared to AK values in healthy brains) tends to depend on the type of microstructural changes that occur in pathological conditions. For example, it decreases in axonal injury but increases with brain maturation.

We found significantly altered RK values in 10 ROIs of the patient group as compared to that of the control group. The anatomical regions include mostly GM-rich ROIs such as frontal gyrus, fronto-orbital gyrus, gyrus rectus, and entorhinal area. Our results overlap with the findings of Tummala *et al*.[17] in which significantly increased RK values in the hippocampus, amygdala, temporal and frontal lobes, insula, midline pons, and cerebellar peduncles of their patient group were reported. Higher RK values are usually indicative of demyelination or dysmyelination. Changes in the axonal diameter or density (number of axons in a bundle) may also influence RK values.

Akkoyunlu *et al*. (2012) found a significant increase in the ADC values in the hippocampus, amygdala, and putamen in OSA patients and concluded that these were likely indicative of hypoxia and vasogenic edema in specific regions of the brain.[13] We found increased MK values in six ROIs including frontal gyrus, fronto-orbital gyrus right, entorhinal region right, and anterior commissure right. Tummala *et al*. have reported significantly increased MK values in the basal forebrain, extending to the hypothalamus, thalamus, insular cortices, basal ganglia, ventral temporal lobe, hippocampus, limbic regions, cerebellar areas, parietal cortices, ventrolateral medulla, and midline pons.[18] Our findings agree well with the results of their study in many regions.

KFA is a summary measure of microstructural complexity in both the axial and radial directions of the WM in the brain. Though it is highly sensitive to microstructural complexity changes, it is less specific to whether the change occurred in axial or radial or both directions of axons. We found altered KFA in multiple brain ROIs including regions in the frontal lobe, cingulate, putamen, globus pallidus, substantia nigra, cerebellar peduncle, and insula. Macey *et al*.[11] studied FA derived from DTI in patients with untreated OSA with AHI more than 15. They found multiple brain regions with lower FA in the OSA group such as the anterior corpus callosum, right column of the fornix, anterior and posterior cingulate cortex and cingulum bundle, portions of the frontal, ventral prefrontal, parietal and insular cortices, bilateral internal capsule, middle cerebellar peduncle, left cerebral peduncle and corticospinal tract, and deep cerebellar nuclei. Though there is no one-to-one agreement between the brain regions shown by their study and our findings, there is a general trend of some brain regions that are common in both the studies. The fact that our study found several altered GM regions in OSA patients illustrates the advantages of using DKI to assess changes in GM regions, too.

Chen *et al*. have calculated various DTI indices and found significantly low FA, increased RD, and no significant difference in AD and MD in the brain of patients with OSA.[12] Our study showed that all DKI indices (i.e., AK, RK, KFA, and MK) were altered in the brain of OSA patients as compared to controls. We performed atlas-based whole-brain analysis that includes GM and WM regions

whereas the above study assessed only WM regions. Castronovo *et al*. have reported decreased FA and MD by DTI analysis in the WM of OSA patients.[14] We found significantly increased KFA and MK in a relatively higher number of anatomical regions of the brain in OSA patients. Our results indicate that the brain tissue structural alterations are more widespread than reported by previous studies. But contrary to above study,[12] we found that changes in MK were more localized to frontal lobes as compared to medullary respiratory regulatory sites. Our results were also similar to Kumar *et al*.[6] who found significant differences in RD and AD in recently diagnosed patients with OSA by using DTI. We found significant changes in 54 and 10 brain ROIs for AK and RK, respectively.

Table 3: MK values which showed a significant difference between patients and control

Area	Patients		Control		*P*
	Mean	Std. deviation	Mean	Std. deviation	
SFG_pole_L	0.651	0.122	0.560	0.075	0.007
SFG_pole_R	0.703	0.150	0.606	0.049	0.012
MFG_DPFC_R	0.746	0.150	0.673	0.036	0.045
MFOG_R	1.064	0.304	0.843	0.128	0.006
ENT_R	0.699	0.098	0.746	0.032	0.046
AnteriorCom_R	0.717	0.156	0.802	0.078	0.036

Table 4: RK values which showed a significant difference between patients and control

Area	Patients		Control		*P*
	Mean	Std. deviation	Mean	Std. deviation	
SFG_pole_L	0.655	0.085	0.559	0.079	0.001
SFG_pole_R	0.689	0.128	0.603	0.056	0.009
MFG_DPFC_L	0.709	0.073	0.657	0.039	0.007
MFG_DPFC_R	0.756	0.125	0.688	0.041	0.030
LFOG_R	0.853	0.175	0.764	0.059	0.043
MFOG_L	0.942	0.107	0.855	0.114	0.016
MFOG_R	1.094	0.267	0.855	0.143	0.001
RG_R	0.793	0.102	0.719	0.092	0.020
ENT_R	0.725	0.043	0.754	0.037	0.034
AnteriorCom_R	0.778	0.082	0.867	0.112	0.007

Our results of significant changes in MK in many ROIs of the brain of patients with OSA agrees with the findings of Kumar *et al*.[7] who found altered MD in the brain of certain anatomical regions in patients with OSA as compared to controls. Furthermore, we found additional anatomical regions with altered MK values that suggest tissue structural alterations due to OSA are more widespread within the brain than reported by other studies using DTI and other MRI techniques. Thus, the brain of patients with OSA can be better evaluated using DKI data.

There are a few limitations to our study. First, we have not compared the DKI parameters of patients with OSA with the DTI parameters of them in this study. Thus, the relative sensitivity of the DKI parameters over the DTI parameters for the evaluation of tissue structural alterations in the brain of patients with OSA could not be ascertained in this study. Second, we could not establish correlation with the neurocognitive impairments in the domains of memory, visual memory, and execution functions with the DKI parameters of the brain of patients with OSA. Since any neurocognitive function is thought to originate or localize in more than one brain anatomical regions and also execution of it requires a coordination between the regions, a different type of advanced data analysis method (e.g., brain network or circuit level and brain connectome-wide analyses) is necessary for the evaluation of the associations between the neurocognitive deficits found in this group of patients and their neuroimaging findings. Large sample size and morphological brain imaging data are also needed for such an analysis, and therefore no attempt was made to do such an analysis in this study.

Conclusions

This prospective study in OSA patients demonstrated significant abnormalities for various DKI parameters using a whole-brain atlas in several brain anatomical regions as compared to controls. Furthermore, DKI data showed significantly more subtle tissue structural abnormalities than other routinely used clinical MRI techniques. Thus, the

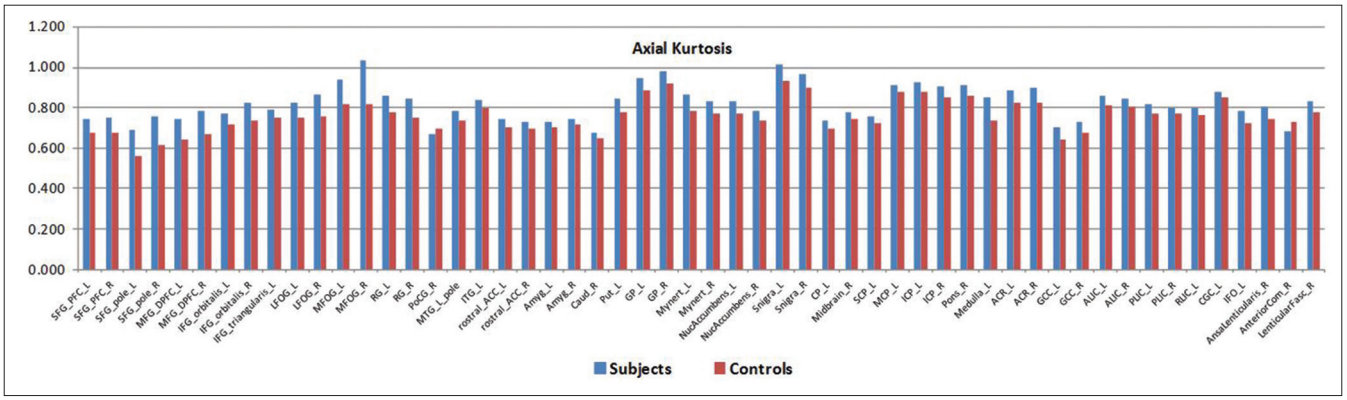

Figure 2: Bar diagram presentation of areas showing significant difference in AK values between patient and control groups

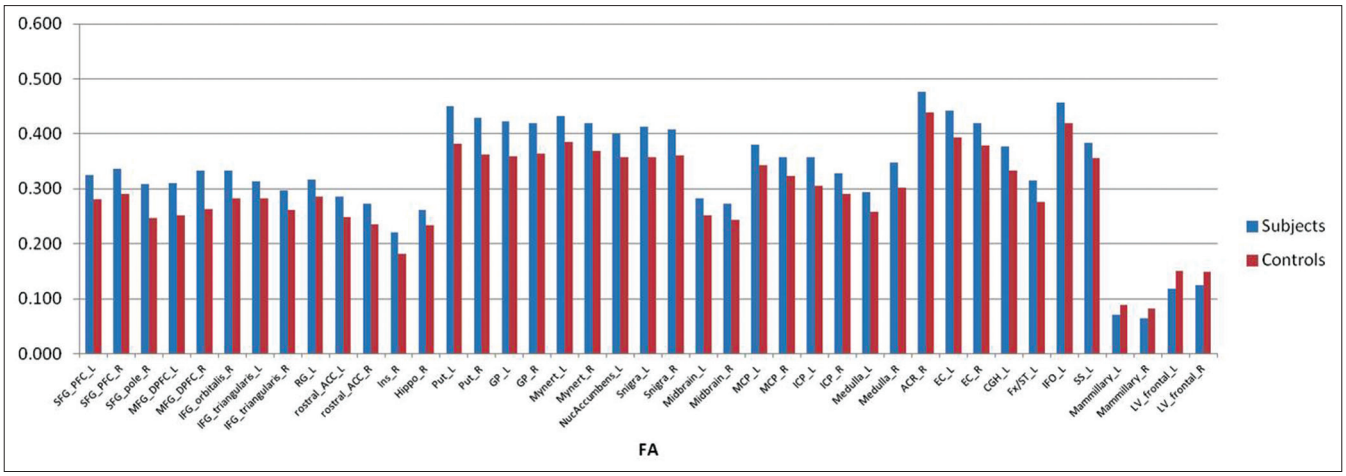

Figure 3: Bar diagram presentation of areas showing significant difference in KFA values between patient and control groups

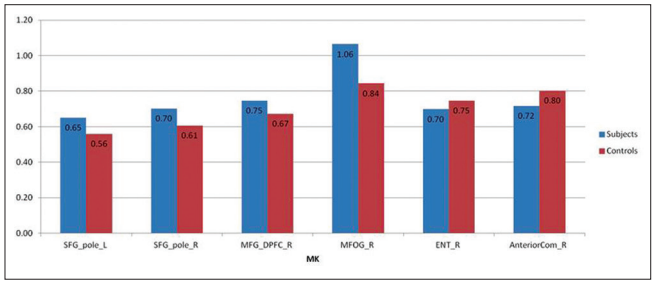

Figure 4: Bar diagram presentation of areas showing significant difference in MK values between patient and control groups

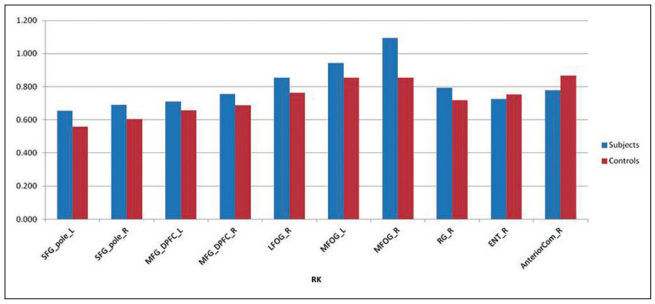

Figure 5: Bar diagram presentation of areas showing significant difference in RK values between patient and control groups

kurtosis parameters are more sensitive in demonstrating tissue structural organization abnormalities at the microstructural level before any detectable changes appear in conventional MRI or other imaging modalities. In addition, DKI showed tissue structural alterations in multiple brain regions, which may be the underlying pathology for the neurocognitive impairments observed in OSA patients. These findings indicate the importance of using DKI for future in-depth studies to evaluate the brain tissue microstructural changes in patients with OSA and associate the changes with their clinical signs or symptoms and cognitive functions.

Ethical approval

All procedures performed in the studies involving human participants were in accordance with the ethical standards of the institutional and/or national research committee and with the 1964 Helsinki Declaration and its later amendments or comparable ethical standards.

Declaration of patient consent

Informed consent was obtained from all individual participants included in the study.

Financial support and sponsorship

Nil.

Conflicts of interest

There are no conflicts of interest.

References

1. Zimmerman ME, Aloia MS. A review of neuroimaging in obstructive sleep apnea. J Clin Sleep Med 2006;2:461-71.
2. Macey PM, Henderson LA, Macey KE, Alger JR, Frysinger RC, Woo MA, *et al*. Brain morphology associated with obstructive sleep apnea. Am J Resp Crit Care 2002;166:1382-7.
3. Morrell MJ, Jackson ML, Twigg GL, Ghiassi R, McRobbie DW, Quest RA, *et al*. Changes in brain morphology in patients with obstructive sleep apnoea. Thora×2010;65:908-14.
4. O'Donoghue FJ, Briellmann RS, Rochford PD, Abbott DF, Pell GS, Chan CH, *et al*. Cerebral structural changes in severe obstructive sleep apnea. Am J Respir Crit Care Med 2005;171:1185-90.
5. Morrell MJ, McRobbie DW, Quest RA, Cummin AR, Ghiassi R, Corfield DR. Changes in brain morphology associated with obstructive sleep apnea. Sleep Med 2003;4:451-4.
6. Kumar R, Pham TT, Macey PM, Woo MA, Yan-Go FL, Harper RM. Abnormal myelin and axonal integrity in recently diagnosed patients with obstructive sleep apnea. Sleep 2014;37:723-32.
7. Kumar R, Chavez AS, Macey PM, Woo MA, Yan-Go FL, Harper RM. Altered global and regional brain mean diffusivity in patients with obstructive sleep apnea. J Neurosci Res 2012;90:2043-52.
8. O'Donoghue FJ, Wellard RM, Rochford PD, Dawson A, Barnes M, Ruehland WR, *et al*. Magnetic resonance spectroscopy and neurocognitive dysfunction in obstructive sleep apnea before and after CPAP treatment. Sleep 2012;35:41-8.
9. Steven AJ, Zhuo J, Melhem ER. Diffusion kurtosis imaging: An emerging technique for evaluating the microstructural

environment of the brain. AJR Am J Roentgenol 2014;202:W26-33.

10. Fieremans E, Jensen JH, Helpern JA. White matter characterization with diffusional kurtosis imaging. Neuroimage 2011;58:177-88.
11. Macey PM, Kumar R, Woo MA, Valladares EM, Yan-Go FL, Harper RM. Brain structural changes in obstructive sleep apnea. Sleep 2008;31:967-77.
12. Chen HL, Lu CH, Lin HC, Chen PC, Chou KH, Lin WM, *et al*. White matter damage and systemic inflammation in obstructive sleep apnea. Sleep 2015;38:361-70.
13. Emin Akkoyunlu M, Kart L, Kılıçarslan R, Bayram M, Aralasmak A, Sharifov R, *et al*. Brain diffusion changes in obstructive sleep apnoea syndrome. Respiration 2013;86:414-20.
14. Castronovo V, Scifo P, Castellano A, Aloia MS, Iadanza A, Marelli S, *et al*. White matter integrity in obstructive sleep apnea before and after treatment. Sleep 2014;37:1465-75.
15. Harper RM, Kumar R, Ogren JA, Macey PM. Sleep-disordered breathing: Effects on brain structure and function. Respir Physiol Neurobiol 2013;188:383-91.
16. Tummala S, Roy B, Park B, Kang DW, Woo MA, Harper RM, *et al*. Associations between brain white matter integrity and disease severity in obstructive sleep apnea. J Neurosci Res 2016;94:915-23.
17. Tummala S, Roy B, Vig R, Park B, Kang DW, Woo MA, *et al*. Non-gaussian diffusion imaging shows brain myelin and axonal changes in obstructive sleep apnea. J Comput Assist Tomogr 2017;41:181-9.
18. Tummala S, Palomares J, Kang DW, Park B, Woo MA, Harper RM, *et al*. Global and regional brain non-gaussian diffusion changes in newly diagnosed patients with obstructive sleep apnea. Sleep 2016;39:51-7.
19. Tabesh A, Jensen JH, Ardekani BA, Helpern JA. Estimation of tensors and tensor-derived measures in diffusional kurtosis imaging. Mag Reson Med 2011;65:823-36.
20. Ceritoglu C, Oishi K, Li X, Chou MC, Younes L, Albert M, *et al*. Multi-contrast large deformation diffeomorphic metric mapping for diffusion tensor imaging. Neuroimage 2009;47:618-27.
21. ROI Editor, Available from: https://www.mristudio.org. [last accessed on 2019 Dec 28].